The chemical characterization and reflectivity of the Al(1.0%wtSi)/Zr periodic multilayer

Qi Zhong, Zhong Zhang, Jingtao Zhu, Zhanshan Wang, Philippe Jonnard, Karine Le Guen, Jean-Michel André

The chemical characterization and reflectivity of the Al(1.0%wtSi)/Zr periodic multilayer

Qi Zhong[1], Zhong Zhang[1,*], Jingtao Zhu[1], Zhanshan Wang[1], Philippe Jonnard[2], Karine Le Guen[2], Jean-Michel André[2]

1 MOE Key Laboratory of Advanced Micro-Structured Materials, Institute of Precision Optical Engineering, Department of Physics, Tongji University, Shanghai 200092, China

2 Laboratoire de Chimie Physique – Matière Rayonnement, UPMC Univ Paris 06, CNRS UMR 7614, 11 rue Pierre et Marie Curie, F-75231 Paris cedex 05, France

Abstract

The reflectivity of Al(1.0%wtSi)/Zr multilayer with 40 periods has been measured in the region of 17nm–19nm. Experimental peak reflectivity is 41.2% at 5° incidence angle. However, the corresponding theoretical value for an ideal Al(1.0%wtSi)/Zr multilayer is 70.9%. In order to explain the difference between theoretical and experimental reflectivity, the multilayer has been characterized by X–ray diffraction and X–ray photoelectron spectroscopy except grazing incident X–ray reflection (GIXR) and cross-sectional transmission electron microscopy. Based on this analysis, the four impact factors responsible for the loss of reflectivity are inhomogeneous crystallization of aluminum, contamination of the multilayer, surface oxidized layer and interdiffusion between Al and Zr layers. The effects of different impact factors on the EUV reflectivity of the Al(1.0%wtSi)/Zr multilayer have been introduced independently by means of corresponding simulations.

Keywords: Al(1.0%wtSi)/Zr multilayer; EUV reflectivity; XPS; interface; simulation

* Corresponding author. Tel.: +86 021 65984652; fax: +86 021 65984652.
E-mail address: zhangzhongcc@tongji.edu.cn

1. Introduction

Aluminum is a promising material for use in extreme ultra-violet (EUV) multilayers operating range from 17nm to 25nm, because it has very low absorption below the Al L-edge. However, the properties of Al-based multilayer mirrors are limited by interdiffusion and inhomogeneous crystallization of aluminum in the EUV spectral range [1–6].

Qadri et al. first studied thick Al/Zr multilayer and found disordered interfaces in the multilayer. Since then, few studies have been published, mainly dealing with the thick multilayer structure [7–10]. Recently, Al/Zr multilayer has shown very promising performance in the EUV region [11, 12]. In our previous paper [11], we found that the Si doping in Al layer could influence the optical performance of Al/Zr system, which could change the crystallization of Al and Zr layers and smooth the interfaces. From the analysis of Al(1.0%wtSi)/Zr periodic multilayer with a large number of periods, it was deduced that the interfacial roughness is small for the first 40 periods toward the substrate, but increases with the period number larger than 40. Experimental peak reflectivity of Al(1.0%wtSi)/Zr multilayer with 40 periods is 41.2% at 5° incidence angle, which is much lower than corresponding theoretical value of 70.9%. The images of transmission electron microscopy (TEM) suggested that the decreasing reflectivity was mainly caused by the variable interfacial roughness in the multilayer. The lack of further data explaining the low experimental reflectivity in the EUV region, made the accurate simulation of Al(1.0%wtSi)/Zr multilayer very difficult.

In this paper, we present a comparison between theoretical and experimental optical performances of Al(1.0%wtSi)/Zr multilayer with 40 periods. After a brief description of the experimental process (Sect. 2), the structural and chemical

characterizations of the multilayer are investigated in Sect. 3 by using X–ray diffraction (XRD) and X–ray photoelectron spectroscopy (XPS). Section 4 deals with simulation of Al(1.0%wtSi)/Zr multilayer reflectivity. We conclude with the impact factors responsible for the loss of reflectivity, and some possible improvements in the Section 5.

2. Experimental Methods

At this place we think relevant to recall the parameter of the prepared multilayer. The Al(1.0%wtSi)/Zr multilayer with 40 periods or bilayers was fabricated by direct–current magnetron sputtering technology [11, 13–17], under the base pressure 8.0×10^{-5}Pa. The sputtering gas was Ar with purity of 99.999%, and the gas pressure was held constantly at 1.35 ±0.02mTorr (0.18Pa). The substrate was fluorine-doped tin oxide coated glass (FTO). The targets of zirconium (99.5%) and silicon doped aluminum (Al(1.0%wtSi)) with diameter of 100 mm were used. The thickness of the multilayer is 9.3nm, and gamma value is 0.33. To characterize the sample, the XRD measurements were used to provide the identification of crystalline phases present in the multilayer.

For XPS characterization, the Al2p, Zr3d, O1s, C1s and Si1s core level spectra were recorded by using the Thermo Scientific ESCALAB 250 spectrometer. The sample was irradiated by an Al K_α monochromatic source (1486.6 eV) and a take-off angle of 90 °. It was analyzed at the surface and after sputtering with a 2kV Ar^+ ion gun (0.16nm/s sputter rate on Ta_2O_5 reference sample). The binding energy scale was calibrated using the reference carbon C1s peak at the binding energy 285eV. With this calibration, the binding energy of the hydrocarbon contamination is 284.9eV.

Reflectivity in the EUV range measured with an incidence angle of 5 ° (near normal incidence) in the Spectral Radiation Standard and Metrology Beamline and Station (beamline U26) at the National Synchrotron Radiation Laboratory in Hefei, China.

3. Results and discussion

3.1 Al(1.0%wtSi)/Zr reflectivity in the region of 17-19nm

From the previous paper [11], the reflectivity and peak position of the multilayer having 40 periods were 41.2% and 17.80nm. Based on Fresnel coefficients, recursion formula and simplex algorithm [18, 19], we design a program to calculate the reflectivity of Al(1.0%wtSi)/Zr periodic multilayer. In the theoretical calculation, the corresponding reflectivity of an ideal multilayer is 70.9% without roughness and interdiffusion (Fig. 1), using the optical constants from Henke et al [20]. The normalized reflectivity decrease (i.e. defined as R(measurement)/R(theory)) of the sample is 0.58. One can realize the important disagreement between theoretical and experimental reflectivity values, which can be attributed to the poor multilayer quality.

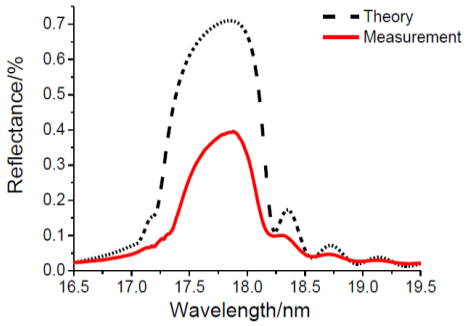

Fig. 1. Theoretical (dashed line) and measured (red line) reflectivity at 17.8 nm of Al(1.0%wtSi)/Zr multilayers at incidence angle of 5 °(near normal incidence).

3.2 X–ray diffraction measurements

From XRD-measurements in the previous paper [11], we can get the crystal orientation and grain size of the Al(1.0%wtSi)/Zr multilayer. Considering the Scherrer formula [21], the grain sizes of Al<111>, Zr<002> and <101> are

6.3±0.2 nm, 5.9±0.2 nm, and 8.7±0.2 nm, respectively. The grain sizes of Zr<002> and <101> are all larger than the Zr thickness (3.17nm), and may represent the in-plane grain size of the Zr layer. The Al<111> grains (i.e. the out-of-plane grain size) [1] grow to a size of 6.3nm equal Al layer thickness (6.2nm). It appears that the Al grain size could be one of the reasons explaining the variable roughness in the grazing incident X–ray reflection (GIXR) simulation [11], participating to the discrepancy between simulated and experimental EUV reflectivity.

3.2.1 Contamination of the multilayer

To get information on the possible compounds formed by Al and Zr materials at the multilayer interfaces, the structure and composition of the Al(1.0%wtSi)/Zr multilayer are characterized by XPS. Fig. 2 shows depth atomic concentration profiles deduced from XPS measurements. The atomic concentration is equal to the weighted average value of the peak integral area in the XPS spectra divided by the corresponding element sensitivity factor. The surface mainly contains Zr, C, O and Si. The carbon on the surface is attributed to the hydrocarbon contamination, which is bonded with O and Zr [22]. But after sputtering 4 min, carbon still remains due to the low ambient condition during the deposition process. The fitting curve of C1s core level spectra (not shown) indicates that the carbon is bonded with Al and Zr in the multilayer. The values of the binding energy (BE) of Al-C and Zr-C components are 285.5 eV and 282 eV, respectively.

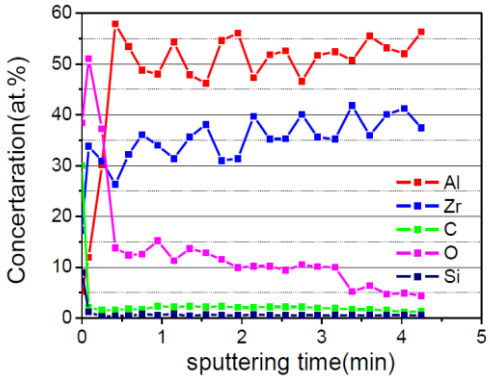

Fig. 2. Atomic concentration of Al, Zr, Si, C and O ratio vs sputtering time.

On the surface, the presence of Si is due to a contamination. Following sputtering, all the Si atoms come from the 1.0 at.% Si doping in Al material (Because Si and Al have similar atom quality, the 1.0 at.% Si could instead of 1.0%wtSi in the multilayer). The atomic concentration of Si does not change with the variable concentration of Al and Zr during sputtering, but remains at 0.5 at.% throughout the multilayer. That suggests Si interdiffusion between the Al and Zr layers in the Al(1.0%wtSi)/Zr system, which also could be the reason why the Si doping in Al layer disfavors the crystallization of Al layer, and promotes the crystallization of Zr layer [11].

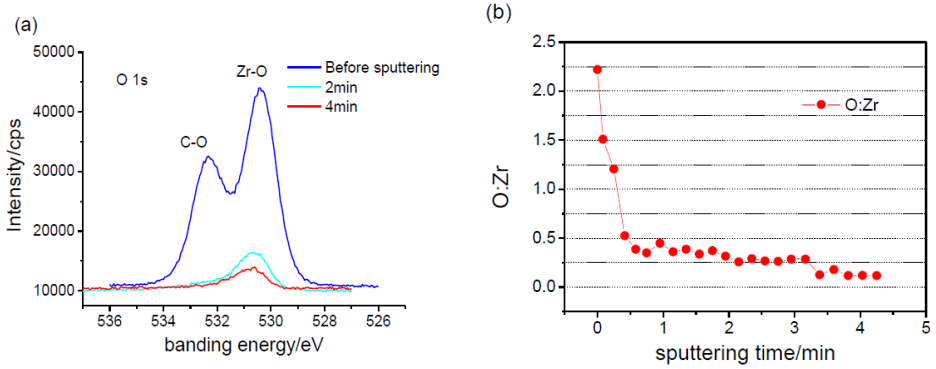

Fig. 3. (a) O1s XPS spectra on before and after sputtering (2 and 4 min); (b) O:Zr ratio vs sputtering time.

Fig. 3(a) shows the surface oxygen O1s peak, which is due to the natural oxidation of the sample. The oxygen is bonded with Zr and C on the surface. The binding energies of Zr–O and C–O components are 530.5eV and 532.4eV, respectively, consistent with the results in the reference [23]. However, following sputtering oxygen is bonded with Al

and Zr, BE=532.1±0.5eV and 530.9±0.5eV for Al–O and Zr–O components. Except for the different intensity of peak, there is no significant difference of the peak shape between the sputtering times of 2 and 4min (Fig. 3(a)). Fig. 3(b) presents the ratio of O to Zr concentration as a function of the sputtering time. Prior sputtering, the O and Zr concentrations correspond to the material ZrO_2. However, the O: Zr ratio decreases with time and reaches 1.2 after 15s sputtering. This may be attributed to the fact that Zr is fully oxidized on the surface, but partly oxidized in the first Zr layer. Considering the sputtering rate, the thickness of the surface zirconium oxide layer, containing ZrO and ZrO_2, can be roughly calculated as 2.4 nm.

3.2.2 Characterization of the interlayer

To decrease the influence of the oxygen contamination, we choose four points (Zr layer, Al–on–Zr layer, Zr–on–Al layer and Al layer) after sputtering time 203s, 229s, 242s and 216s, respectively. The Al and Zr core level spectra are shown in Fig.4. In Fig. 4(a), the $Zr3d_{5/2}$ binding energy obtained in the free Zr, the two interface materials (Al–on–Zr and Zr–on–Al) and free Al are 178.4 eV, 178.8 eV, and 178.6 eV, respectively. The same situation (BE shift as a function of the analyzed layer) appears in Al2p spectra (Fig. 4(b)). Considering the results in the Fig.4, we can find that there are different binding energies of Al and Zr in one period owing to the large interdiffusion between Al and Zr layers. Therefore, we will use two interlayers (Al–on–Zr and Zr–on–Al) with the same material and thickness to represent the interdiffusion in the multilayer. Thus, instead of the original two–layer model [8, 11], a four-layer model will be used to characterize the structure of the Al(1.0%wtSi)/Zr sample.

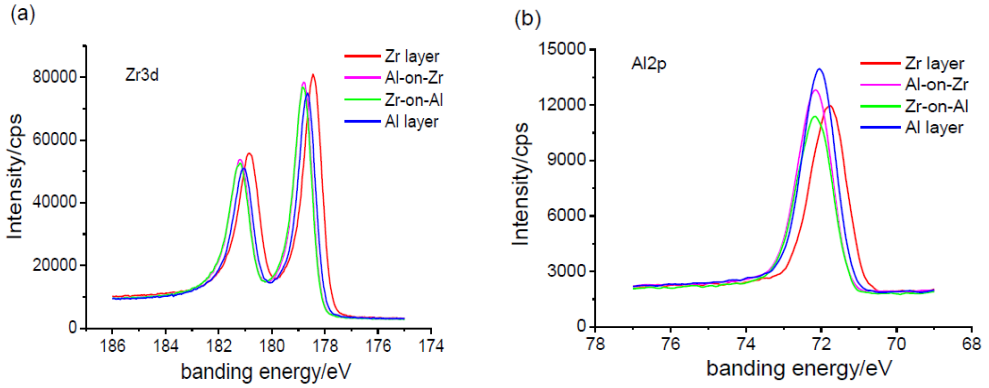

Fig. 4. Zr3d (a) and Al2p (b) XPS spectra of four points after sputtering time 203s (Zr layer), 229s (Al-on-Zr layer), 242s (Zr-on-Al layer) and 216s (Al layer) respectively.

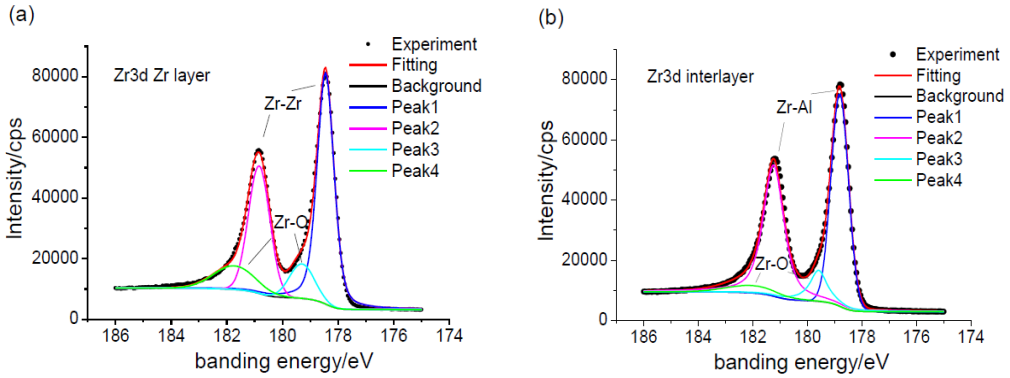

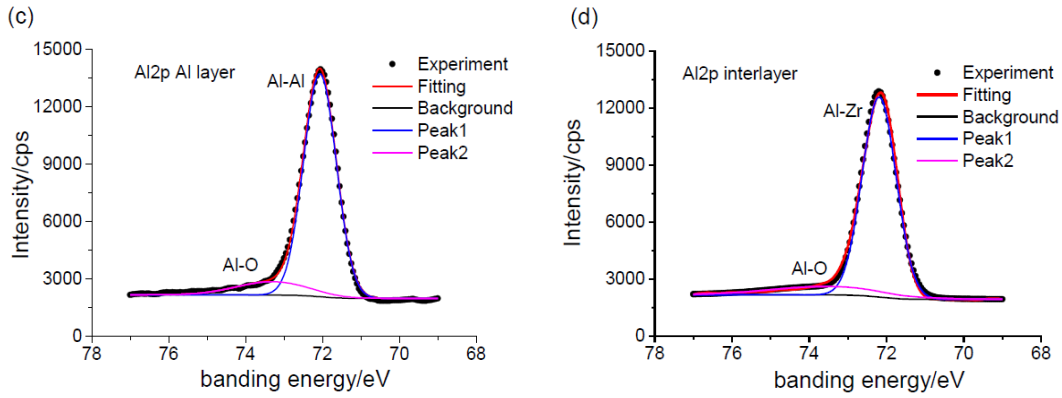

Fig. 5. Fits of the Al interlayer and Zr layer in Zr3d (a, b) and Al 2p (c, d) spectra, black points: experiment results, red lines: recomposing signal, color lines: components obtained from the decomposition of the core level.

From curves fitting, both the shape and BE (178.4 eV) of the Zr $3d_{5/2}$ core level do not correspond to those of Zr metal (177.9 eV) [24] in the Zr layer (Fig. 5(a)). This may suggest that Zr is little oxidized, but forms neither the material ZrO nor ZrO_2 in the Zr layer. In Fig. 5(b), the BE of the Zr 3d5/2 in the interlayer shifts to 178.8 eV, matching the metallic state of zirconium in the alloys [24]. The Al 2p spectrum of the Al layer (Fig. 5(c)) presents the only curve of low intensity containing Al–Al and Al–O bond, located at 72.0 and 73.6eV, respectively. In the interlayer (Fig. 5(d)), the BE of Al 2p bond is at 72.2eV, characteristic of metallic aluminum [23, 25]. In summary, we found that the interlayer presents a metallic state different from that of the Al and Zr metal layers and that all the layers are slightly oxidized. To estimate the composition of $ZrAl_x$ alloy in the interlayer (x represents the Al: Zr ratio), the Zr and Al concentrations and Al: Zr ratio as a function of the sputtering time are shown in Fig. 6. As an example, the x values of the two interlayers of the 6^{th} period, which sputtering time is 229s and 242s, are 1.33 and 1.26, respectively. The difference of the x values may be attributed to gradual change of interdiffusion in the interface and to the experimental uncertainty. Considering many forms of Al-Zr alloy and large interdiffusion in the multilayer, we assume the ratio (x=1.33) of the interlayer can represent the common situation in the interface boundary, which will be convenient for the simulation in the following section.

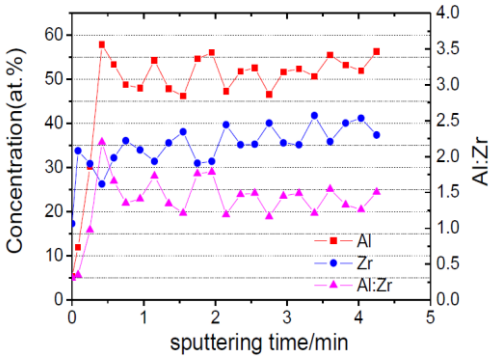

Fig.6. Zr and Al atomic concentrations of and Al: Zr ratio vs sputtering time.

4 Simulation

We have extracted different impact factors from the analysis of the XRD and XPS measurements, namely inhomogeneous crystallization of aluminum, contamination of the multilayer, surface oxidized layer and interdiffusion between Al and Zr layers. For the contamination in the multilayer, we could improve the vacuum condition, which is not involved in the following simulation. Therefore, the other three effects are considered in the simulated reflectivity. By using the EUV reflectivity program mentioned above, we introduce those three factors step by step into the ideal multilayers. Those effects are the following:

- (1) For the inhomogeneous crystallization of aluminum, we use the interfacial roughness to represent the effect between the different layers. The values are changed from 0.7nm (substrate) to 0.4nm (surface) result of the GIXR simulation in previous paper [11].
- (2) A four–layer model is used for the simulation. We calculate the reflectivity with 1.5 nm of interlayer at each interface [12], and use the $ZrAl_{1.33}$ to represent the material stoichiometry.
- (3) The oxidation of the Zr top layer ($ZrO_{1.5}$) is confirmed by XPS measurements. The thickness of oxidized layer is 2.4nm. Using the surface roughness in the AFM [11], the value is 0.4nm.

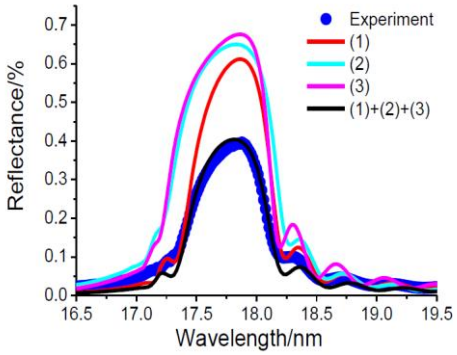

Fig.7. Comparison of measured and simulated reflectivity values for Al(1%wtSi)/Zr. Simulation results from individual or combined simulation cases are derived from Table 3.

We calculate the three factors independently, and the combined effect of the three modifications (1) + (2) + (3) in Fig. 7. In Table 1, the reflectivity values corresponding to the factors (1), (2) and (3) are 61.2%, 64.9% and 67.6%, respectively, that is to say higher than the experimental value of 41.2%. However, combining the three factors (1) + (2) + (3), the agreement between simulated (40.8%) and experimental reflectivity is good. We can conclude that all the factors responsible for the loss of reflectivity.

Table 1. Comparison of experimental and simulated reflectivity values (R) at 17.8nm for Al(1.0%wtSi)/Zr in different impact factors.

Sample	**Al(1.0%wtSi)/Zr**
R% exp.	41.2
R% theory	70.9
R% (1)	61.2
R% (2)	64.9
R% (3)	67.6
R% (1)+(2)+(3)	40.8

5 Conclusion

We report a comparative study of theoretical and experimental performances of Al(1.0%wtSi)/Zr multilayers made of 40 periods. The Al(1.0%wtSi)/Zr have been characterized by several techniques. XRD analysis of the Al(1.0%wtSi)/Zr shows that the grain size of Al is 6.3nm in the sample, which could be responsible for the roughness at the interface. Based on the XPS measurements, Zr in surface of the multilayer is oxidized (about 2.4 nm of ZrO_x). Not only oxygen atoms, but also the carbon atoms can reach into the Zr and Al layers of the multilayer. We find that Si can influence crystallization of the metal layer through its interdiffusion from Al to Zr layer. The composition of interlayer is close to the one of the Al–Zr alloy, $ZrAl_{1.33}$, which we use to represent the compounds in the interface.

In order to identify the differences between theoretical and experimental reflectivity, the impact factors have been introduced in the reflectivity simulation. We found that the four factors responsible for the loss of reflectivity are the inhomogeneous crystallization of aluminum, contamination of the multilayer, surface oxidized layer and interdiffusion between Al and Zr layers. Some improvements can be envisaged. Considering the experimental point of view, we can use

the different doping in Al layer to disfavor the crystallization and improve vacuum condition to decrease the contamination. To reduce the influence of zirconium oxide layer, a capping layer is needed, which should lead to optimize the thickness of the layer just under the capping layer [26]. Another way to improve the reflectivity would be adding a barrier layer between the Al and Zr layers to prevent the interdiffusion.

Acknowledgement

This work is supported by National Basic Research Program of China (No. 2011CB922203) and National Natural Science Foundation of China (No.10825521, 11061130549).

References

[1] D.L. Windt, J.A. Bellotti, Performance, structure, and stability of SiC/Al multilayer films for extreme ultraviolet applications, Applied Optics 48 (26) (2009) 4932–4941.

[2] P. Jonnard, K. Le Guen, M.-H. Hu, J.-M. Andr é, E. Meltchakov, C. Hecquet, F. Delmotte, A. Galtayries, Optical, chemical and depth characterization of Al/SiC periodic multilayers, Proceeding of SPIE 7360 (1997) 73600O–1–9.

[3] M-H. Hu, K. Le Guen, J-M Andr é, P. Jonnard, E. Meltchakov, F. Delmotte, A. Galtayries, Structural properties of Al/Mo/SiC multilayers with high reflectivity for extreme ultraviolet light, Optics Express 18 (19) (2010) 20019–20028.

[4] E. Meltchakov, C. Hecquet, M. Roulliay, S.D. Rossi, Y. Menesguen, A. J érome, F. Bridou, F. Varniere, M.-F. Ravet-Krill, F. Delmotte, Development of Al–based multilayer optics for EUV, Applied Physics A 98 (2010) 111–117.

[5] H. Nii, M. Niibe, H. Kinoshita, Y. Sugie, Fabrication of Mo/Al multilayer films for a wavelength of 18.5nm, Journal of Synchrotron Radiation 5 (1998) 702–704.

[6] H. Nii, M. Miyagawa, Y. Matsuo, Y. Sugie, M. Niibem, H. Kinoshita, Control of Roughness in Mo/Al Multilayer Film Fabricated by DC Magnetron Sputtering, Japanese Journal of Applied Physics 41 (2002) 5338–5341.

[7] S.B. Qadri, C. Kim, M. Twigg, D. Moon, Ion–beam deposition of Zr–Al multilayers and their structural properties, Surface & Coating Technology 54 (55) (1992) 335–337.

[8] J.-K. Ho, K.-L. Lin, The Structure of Compositionally Modulated Al-Zr Multilayer films, Scripta Metallurgica of Materialia 33 (12) (1995) 1895–1990.

[9] J.-K. Ho, K.-L. Lin, The metastable Al/Zr alloy thin films prepared by alternate sputtering Deposition, Journal of Applied Physics 75 (5) (1994) 2434–2440.

[10] K.J. Blobaum, T.P. Weihs, T.W. Barbee, Jr., M.A. Wall, Solid state reaction of Al and Zr in Al/Zr multilayers: a calorimetry study, UCRL J C–118965 (1995).

[11] Qi Zhong, Wenbin Li, Zhong Zhang, Jingtao Zhu, Qiushi Huang, Chuanchun Yang, Zhanshan Wang, P. Jonnard, K. Le Guen, J.-M. Andr é, Hongjun Zhou, Tonglin Huo, Optical and structural performance of the Al/Zr reflection multilayers in the 17-19nm region, Optics Express 20 (10) (2012) 10692–10700.

[12] D.L. Voronov, E.H. Anderson, R. Cambie, S. Cabrini, S.D. Dhuey, L.I. Goray, E.M. Gullikson, F. Salmassi, T. Warwick, V.V. Yashchuk, and H.A. Padmore, A 10,000 groove/mm multilayer coated grating for EUV spectroscopy, Optics Express 19 (7) (2011) 6320–6325.

[13] Zhu Jingtao, Huang Qiushi, Bai Liang, Jiang Hui, Xu Jing, Wang Xiaoqiang, Zhou Hongjun, Huo Tonglin, Wang Zhanshan, Chen Lingyan, Manufacture and measurement of SiC/Mg EUV multilayer mirrors in different base pressures, Optics and Precision Engineering 17 (12) (2009) 2946–2951 (In Chinese).

[14] Wang Fengli, Wang Zhanshan, Zhang Zhong, Wu Wenjuan, Wang Hongchang, Zhang Shumin, Qin Shuji, Chen Lingyan, W/B4C、W/C、W/Si multilayers, Optics and Precision Engineering 13 (1) (2005) 28–33 (In Chinese).

[15] Wang Zhanshan, Effect of film thickness errors on performance of soft X-ray multilayer [J], Optics and Precision Engineering 11 (2) (2003) 136–138 (In Chinese).

[16] Xu Yao, Wang Zhanshan, Xu Jing, Zhang Zhong, Wang Hongchang, Zhu Jingtao, Wang Fengli, Wang Bei, Qin Shuji, Chen Lingyan, Characterization of low-Z material layer profiles in bilayer structures by X-ray reflectivity measurement, Optics and Precision Engineering 15 (12) (2007) 1838–1843.

[17] Wu Wenjuan, Wang Zhanshan, Qin Shuji, Wang Fengli, Wang Hongchang, Zhang Zhong, Chen Lingyan, Xu Xiangdong, Fu Shaojun,

Etching of multilayer grating using a narrow spectral band X-ray, Optics and Precision Engineering 12 (2) (2004) 226–230 (In Chinese).

[18] Wang Hongchang, Wang Zhanshan, The Optimzing and Designing Method of Multilayer Film, Journal of Applied Optics 26 (5) (2005) 50–53 (In Chinese).

[19] Zhang Zhong, Wang Zhanshan ,Qin Shuji ,Wang Fengli ,Chen Lingyan, The Design of X-ray Supermirror with Broad angle Range, [J]. Acta Photonica Sinica 32 (2) (2003) 253–256 (In Chinese).

[20] B.L. Henke, E.M. Gullikson, J.C. Davis, X-ray interactions: photoabsorption, scattering, transmission, and reflection at E=50–30000 eV, Z=1-92, Atomic Data and Nuclear Data Tables 54 (2) (1993) 181–342, http://henke.lbl.gov/optical_constants/.

[21] S. Naseer, F.U. Khan, N.U. Rehman, A. Qayyum, F. Rahman, M. Zakaullah, Plasma nitriding of aluminium in a pulsed dc glow discharge of nitrogen, European Physical Journal Applied Physics 49 (2010) 21001–1–7.

[22] A.K. Bhattacharya, D.R. Pyke, R. Reynolds, G.S. Walker, C.R. Werrett, The use of O ls charge referencing for the X-ray photoelectron spectroscopy of Al/Si, Al/Ti and Al/Zr mixed oxides, Journal of Materials Science Letters 16 (1997) 1–3.

[23] V.N. Zhitomirsky, S.K. Kim, L. Burstein, R.L. Boxman, X-ray photoelectron spectroscopy of nano-multilayered Zr–O/Al–O coatings deposited by cathodic vacuum arc plasma, Applied Surface Science 256 (2010) 6246–6253.

[24] X.-Y. Li, E. Akiyam, H. Habazaki, A. Kawashima, K. Asami, K. Hashimoto, An XPS Study of passive films on corrosion resistant Cr–Zr Alloys prepared by sputter deposition, Corrosion Science 39 (8) (1997) 1365–1380.

[25] K. Ichimura, M. Matsuyama, K. Watanabe, Alloying effect on the activation processes of Zr–alloy getters, Journal of Vacuum Science & Technology A 5 (2) (1987) 220–225.

[26] Chen Rui, Wang Fengli, Zhu Jingtao, Wang Hongchang, Wang Zhanshan, Design of 30.4 nm multilayer based on genetic algorithms, Acta Photonica Sinica 37 (9) (2008) 1819–1824 (In Chinese).